STUDIA UBB CHEMIA, LXIX, 1, 2024 (p. 17-34)
(RECOMMENDED CITATION)
DOI:10.24193/subbchem.2024.1.02

HYDROTHERMAL CARBONIZATION OF DECIDUOUS WOODY BIOMASS: PATH TO ENERGY INTENSIFICATION AND FINE CHEMICALS

Mothil SENGOTTIAN[a,*], Chitra Devi VENKATACHALAM[b], Sathish Raam RAVICHANDRAN[a], Sarath SEKAR[b]

ABSTRACT. Four deciduous woody feedstocks (*Casuarina equisetifolia L., Eucalyptus globulus, Wrightia tinctoria*, and *Neolamarika cadamba*) were subjected to the Hydrothermal Carbonization (HTC) process inside a 50 mL stainless steel hydrothermal reactor at varying temperatures (180°C, 215°C, and 250°C), while keeping water-to-feedstock ratio (6:1 v/w%) and residence time (1.5 h) constant. The mass yield and energy yield of the resulting biomass were calculated as parameters for energy intensification. Characterization of the biomass, biochar, and bio-oil was conducted using elemental analysis, SEM, and GC–MS. Interestingly, the mass yield of biochar decreased with increasing temperature, but it significantly improved the energy densification ratio, with a minimum of 1.06 observed for *Neolamarika cadamba* biomass at 180°C and a maximum of 1.23 observed for *Eucalyptus globulus* biomass at 250°C. Moreover, detailed analysis of the bio-oil obtained at 250°C using GC-MS revealed the presence of a diverse range of fine chemicals, including benzyl, carboxylic acid, ester, methyl, phenol, pyrrole, nitro, and aliphatic hydrocarbons. These findings suggest that the HTC process can be optimized to tailor the production of specific value-added chemicals from lignocellulosic woody biomass.

Keywords: *Hydrothermal carbonization (HTC), Biomass, Bio-oil, Biochar, Fine chemicals*

[a] *Department of Chemical Engineering, Kongu Engineering College, Erode-638060, Tamil Nadu, India*
[b] *Department of Food Technology, Kongu Engineering College, Erode-638060, Tamil Nadu, India*
* *Corresponding author smothil666@gmail.com*

INTRODUCTION

Biomass refers to the organic matter derived from plants and animals including the wastes generated out of them [1]. Utilization of this effectively as a resource for energy, heat production, and value added products and chemicals are done through various energy production and intensification process. The search for effective, sustainable and non-polluting technology has never ended and each of them has its own merits and demerits. The main problem during this conversion is the non-uniformity in composition, availability of the resource in a continuous manner, pretreatment of the feedstock and purity of products obtained [2]. Some of the technologies that has been developed by the primitive humans and they are being fine-tuned ever since via both biochemical and thermochemical pathways. The biochemical methods include: extraction, hydrolysis followed by trans-esterification or fermentation resulting in bioethanol and other products [3]. The thermochemical methods include: combustion, gasification, pyrolysis, carbonization and hydrothermal treatment [4,5]. The hydrothermal treatment is the main concern in this study and the focus is given to especially hydrothermal carbonization of selective species of lignocellulosic woody biomass.

Hydrothermal Carbonization (HTC) involves thermal degradation of biomass under subcritical water environment at high temperatures (180 to 250°C) and pressures (2 to 10 MPa) for several hours [6]. This process mimics the natural coalification that takes several hundred years to form peat and million years to form coal, but it only takes a few hours to yield biochar with properties similar to brown coal [7]. HTC is an exothermic reaction and is characterized by the production of solid carbonaceous material called biochar or hydrochar, as well as special chemicals in the form of liquid or dissolved in the residual water through hydrolysis of the biomass. Some of the chemicals produced include organic acids, furfural, and furanoid derivatives [8]. HTC holds significant importance in the production of high-quality biochar with special properties used in pollution control, as adsorbents for removing heavy metals [8, 9] and dyes [10, 11], soil remediation [13], energy generation [14], storage [15] and many other applications.

This study was conducted to gain insights into the reaction mechanism and chemistry underlying the hydrothermal carbonization of lignocellulosic biomass. The primary constituents of plant cell walls are lignocellulose, consisting of layers of cellulose microfibrils, hemicellulose, pectin, and lignin arranged in a uniform structure [16]. Additionally, plant cell walls contain proteins, soluble extractives in smaller amounts, and non-structural materials, such as sugars, nitrogenous compounds, waxes, chlorophyll, and ash [17].

Lu X et al. investigated the hydrothermal carbonization of cellulose at temperatures ranging from 225°C to 275°C, with reaction times between 0.5 to 4 hours. They reported faster conversion at higher temperatures, leading to increased cellulose solubilization and lower wt% of solids with sp2 carbons (furanic and aromatic groups) and alkyl groups [18]. HTC of hemicellulose substitute (D-xylose) exhibited a high hydrochar yield of 50 wt% at 225°C, which slightly decreased at 265°C due to dehydration and decarboxylation, with the formation of furfural as an important intermediate [19]. *Kim D et al.* observed a modest increase in energy densification and high heating value (HHV), but temperatures between 250°C and 280°C favored faster decomposition of lignin, resulting in improved energy densification of 28% and fixed densification of 55% compared to feedstock composition [20].

The chemical composition of biomass can vary from one plant species to another, impacting the yield of HTC products. Although the chemical reactions of the three main model compounds: cellulose, hemicellulose, and lignin are well-defined, the interactions of intermediate reaction species of these individual compounds vary with each biomass, leading to a diverse range of products [21, 22]. Thus, this study aims to explore different woody species of biomass: *Casuarina equisetifolia L. (CE), Eucalyptus globulus (EG), Wrightia tinctoria (WT)*, and *Neolamarika cadamba* (NC) to establish relationships between their constituent ratios, yield, obtain optimized conditions for hydrothermal carbonization and identify the constituents present in the bio-oil obtained.

RESULTS AND DISCUSSION

The physical properties of woody species are listed in Table 1 which was obtained from: Research Wing, Tamil Nadu Forests Department, Chennai. The woody species were chosen based on the wide differences in their morphology, physical properties, and internal tissue structure, as shown in Figure 1.

Table 1. Physical Properties of raw biomass for four wood species

Deciduous Tree Species	Density kg/m^3	Modulus of elasticity kgf/cm^2	Modulus of Rupture kgf/cm^2	Hardness & Grain structure
CE	693	1,14,400	732	Hard to very hard with straight grains
EG	678	99,400	1312	Moderately hard with straight to slightly interlocked grains
ET	570	98,560	946.3	Moderately Hard with even grains
NC	463	95,200	884.1	Soft, Light and Even grained

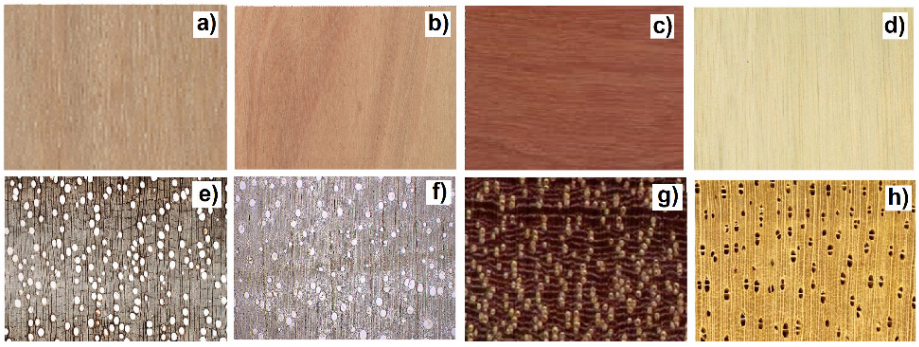

Figure 1. Wood Macroscopic Tangential Section (Polished) a) *CE* b) *EG* c) *WT* d) *NC, Wood Microscopic Transverse Section* - e) *CE* f) EG g) WT h) NC (Adopted from Richter, H.G., Gembruch, K., and Koch, G. 2014 onwards. CITESwoodID: descriptions, illustrations, identification, and information retrieval. In English, French, German, and Spanish. Version: 17th February 2019. delta-intkey.com)

The chemical constituents and the proximate analysis results are presented in Table 2. Although there is no direct relationship between these two sets of data, they were considered to aid in comprehending the hydrothermal carbonization of the four deciduous wood species. It's crucial to emphasize that the composition of chemical constituents in biomass can undergo significant variations influenced by several factors. These include the type of biomass, plant species, growth processes and conditions, plant age, doses of fertilizers and pesticides applied, harvest timing, collection methods, potential contamination, transportation, storage, processing, and other contributing factors [29]. However, in the context of this study, the findings were derived from tree cuttings (12 cm in diameter and 50 cm in length) sourced from the Forest College & Research Institute, Tamil Nadu Agricultural University, Mettupalayam.

Table 2. Chemical Constituents for four wood species

Species	Holo-cellulose (%)	Lignin (%)	Extractives (%)	Ash (%)	Moisture (%)	Fixed Carbon (%)	Volatile (%)
CE	68	39.5	7.5	0.3	10.8	16.4	72.5
EG	66.2	27.7	6.1	0.4	2.28	13.89	83.44
WT	70.1	22.1	7.8	0.65	1.1	17.8	80.45
NC	85.47	31.24	2.45	0.55	9.06	18.4	71.99

The structural characteristics of raw wood, as outlined in Table 1, evidently hinge on the chemical constituents present. Holocellulose, encompassing both cellulose and hemicellulose, in conjunction with lignin, assumes a crucial role in constituting the fundamental building blocks of the wood's cell wall. A higher lignin percentage contributes to denser wood with enhanced flexural properties. Meanwhile, cellulose, hemicellulose (xyloglucan), and pectin are essential for both inherent strength and the capacity to respond to cell expansion during growth. The interplay between hemicellulose and cellulose networks provides a harmonious blend of extensibility and strength, vital for primary cell walls, a balance unattainable with cellulose alone [30].

Table 2 distinctly illustrates notable differences in chemical constituents among various wood species, facilitating a comprehensive examination of their impact on hydrothermal carbonization. Fig 2 presents a comparative analysis of the chemical constituents of wood obtained through proximate analysis, juxtaposed with its pure chemical components and other energy-intensive products such as lignite and coal [20] [31].

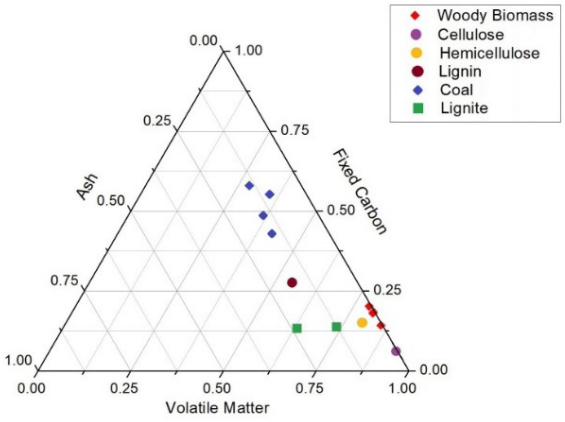

Figure 2. Proximate Analysis of Woody Biomass Feedstock: Comparing Constituents and Energy-Intensive Products.

Hydrothermal carbonization and Energy intensification

Figure 3 shows the biochar obtained during the HTC process. In Figure 4, the yields of hydrothermal carbonization (HTC) products, including biochar, bio-oil, and biogas, are depicted for four biomass species: *Casuarina equisetifolia L., Eucalyptus globulus, Wrightia tinctoria,* and *Neolamarika cadamba*. The experiments were conducted at various temperatures (180°C, 215°C, and 250°C), maintaining a consistent reaction time of 1.5 hours and a water-to-feedstock ratio of 6:1.

The hydrothermal carbonization (HTC) on the four biomass feedstocks revealed similar trends at 180°C and 215°C, whereas at 250°C, there was a decrease in biochar yield accompanied by an increase in biooil production. Casuarina equisetifolia L. and Eucalyptus globulus exhibited similarities to other coniferous trees like pine and spruce. In contrast, Wrightia tinctoria and Neolamarika cadamba displayed a notable increase in biooil yield, attributed to the higher content of crystalline hemicellulose in the softwood species. The important parameters for hydrothermal carbonization, such as mass yield, energy densification ratio, and energy yield, were calculated using equations (3, 4, and 5), with the results presented in Table 3.

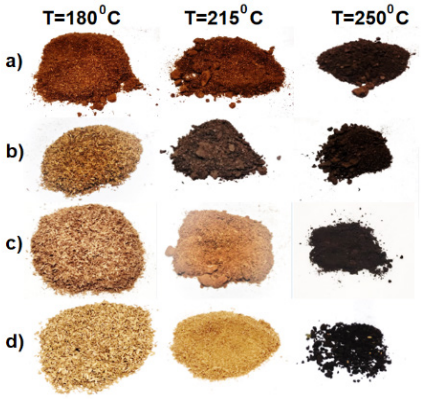

Figure 3. Biochar after HTC -*a) Casuarina equisetifolia L. b) Eucalyptus globulus c) Wrightia tinctoria d) Neolamarika cadamba*

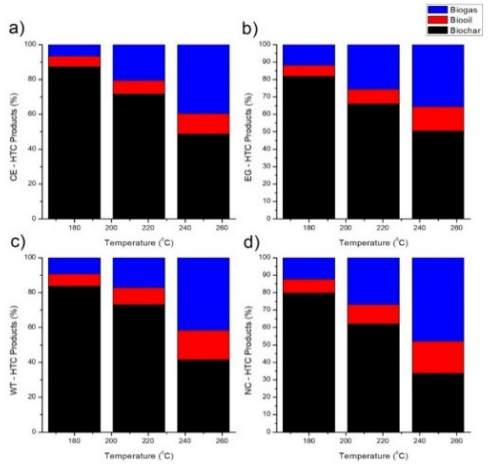

Figure 4. Effect of temperature and yield of HTC products -
a) *Casuarina equisetifolia L.* b) *Eucalyptus globulus* c) *Wrightia tinctoria* d) *Neolamarika cadamba*

Table 3. Energy intensification of HTC products

Species	Temperature (°C)	C (%)	H (%)	N (%)	O (%)	HHV $MJkg^{-1}$	MY (%)	EDR	EY (%)
CE	30	43.8	5.8	0.28	45.37	14.08			
	180	49.4	5.1	0.13	43.20	17.33	87.33	1.11	97.29
	215	52.5	4.2	0.10	39.22	17.64	71.67	1.13	81.24
	250	58.2	2.5	0.08	33.39	18.14	48.67	1.17	56.75
EG	30	42.4	6.1	0.12	51.37	13.91			
	180	48.3	5.4	0.10	46.20	17.19	81.67	1.12	91.66
	215	56.1	3.5	0.09	40.31	18.45	66.00	1.20	79.47
	250	59.7	2.5	0.09	37.71	18.86	50.33	1.23	61.97
WT	30	43.2	6.0	0.62	50.20	14.25			
	180	47.5	5.3	0.47	46.73	16.72	83.67	1.07	89.63
	215	53.4	4.1	0.43	42.07	17.98	73.00	1.15	84.06
	250	60.8	2.1	0.41	36.69	18.90	41.33	1.21	50.05
AC	30	44.5	6.4	0.31	48.80	15.46			
	180	49.9	5.2	0.32	44.58	17.72	79.67	1.06	84.60
	215	54.2	3.9	0.30	41.61	18.08	62.00	1.08	67.17
	250	62.5	1.8	0.28	35.42	19.31	33.67	1.16	38.95

Table 3 presents the fuel properties of HTC biochar, indicating a noticeable increase in the Higher Heating Value (HHV) with higher temperatures. Concurrently, as the temperature increased, the mass yield of biochar decreased while the energy densification demonstrated improvement. Specifically, Neolamarika cadamba biomass showed a minimum energy densification of 6% at 180°C, while Eucalyptus globulus biomass exhibited the highest energy densification of 23% at 250°C. Figure 5 depicts the Van Krevelen diagram, which enables a meaningful comparison of biomass feedstock, biochar at different temperatures, and energy intensified reference products like lignite, coal, and coke.

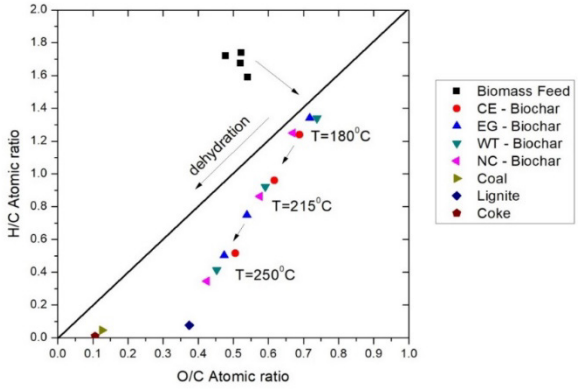

Figure 5. The Van Krevelen diagram of biomass at three HTC reaction temperatures in comparison with energy intensified reference products

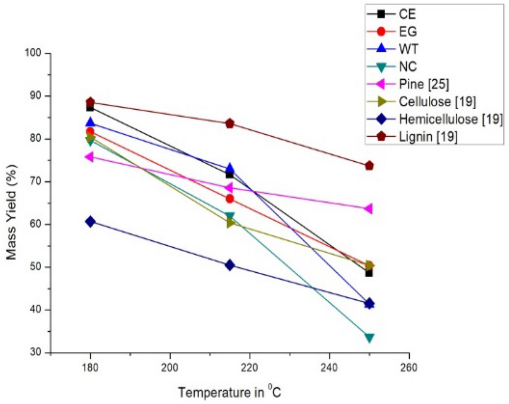

Figure 6. Mass yield in comparison with that of obtained from pure components

An intriguing observation is the significant dehydration effect during HTC compared to conventional coalification processes. In Figures 6 and 7, the mass yield and energy yield of the four deciduous biomass species are depicted at various reaction temperatures (180°C, 215°C, and 250°C). These results are compared with their pure components and simulated outcomes from correlations developed for coniferous pine species, as presented in Equations 6 and 7, respectively [20] [28].

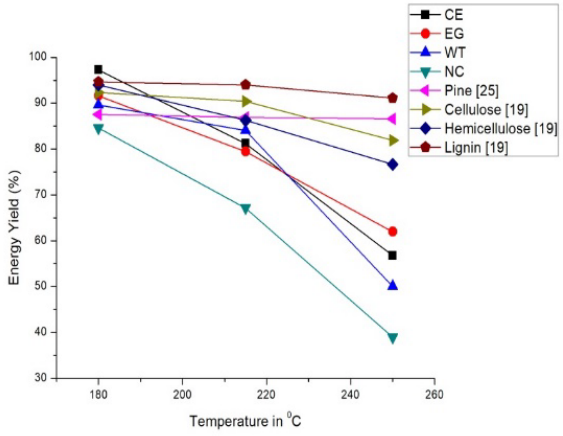

Figure 7. Energy yield in comparison with that of obtained from pure components

The SEM analysis was conducted on the selected biomass (Eucalyptus globulus) resulting from HTC at different temperatures (180°C, 215°C, and 250°C) under constant reaction time (1.5 hours) and a consistent water to feedstock ratio of 6:1. Figure 8 a) depicts the biochar obtained at 180°C at

x150 magnification, indicating the initiation of carbonization with the biomass beginning to flake on the surface. Similarly, Figure 8 b) illustrates the biochar at 215°C, where the biomass is further broken down into smaller particles (250 μm) compared to the previous condition. While in Figure 8 c), the biochar particles at 250°C show further intensification to a size of 50 μm.

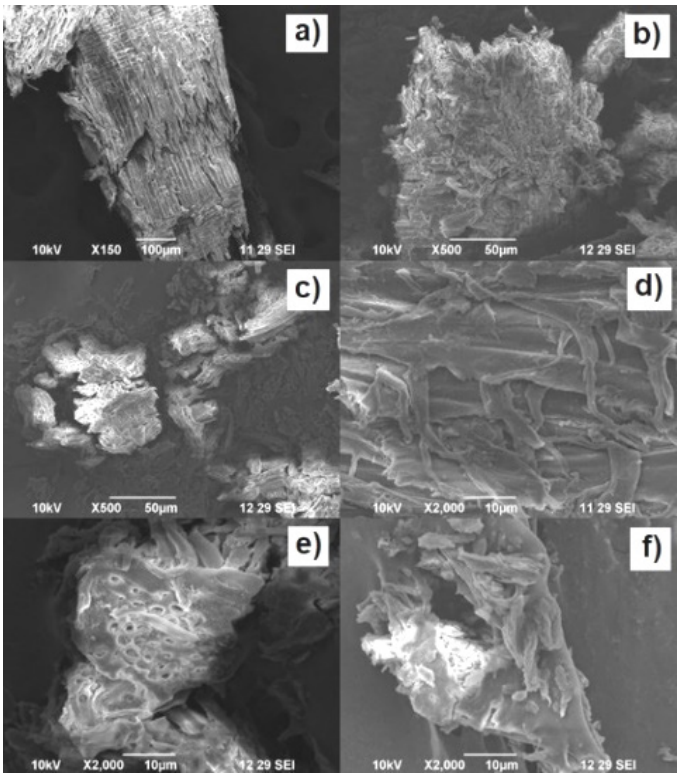

Figure 8. SEM Image of *Eucalyptus globulus* - HTC biochar a) 180°C at x150, b) 215°C at x500, c) 250°C at x500, d) 180°C at x2000, e) 215°C at x2000, f) 250°C at x2000

Figure 8 d), e) and f) shows thermally disintegrated biomass at higher magnification (x2000) at temperatures 180°C, 215 °C and 250 °C respectively. Figure 8 d) shows that the exterior fibres of the woody biomass are observed to be disintegrated. Figure 8 e) shows the transverse section of the biochar with enlarged vessels and this indicate that the reaction is not solely oriented inward but also outward from the vessels. Figure 8 f) reveals a completely modified surface with amorphous lumps.

Chemical characterization of bio-oil from HTC

The experimental results indicated that the highest biooil yield was observed at 250°C. The composition of the bio-oil obtained from the four deciduous feedstocks was analyzed using Gas Chromatography-Mass Spectrometer (GC-MS), and the detailed analysis results are presented in Table 4.

Table 4 Chemical constituents in HTC bio-oil

	Retention Time (min)	Area (%)	Molecular Formula	Average Mass (Da)	IUPAC Name
CE	7.17	1.510	$C_{20}H_{32}O_3$	320.46	Benzyl oxy tridecanoic acid
	13.25	1.578	$C_{20}H_{32}O_3$	320.46	Benzyl oxy tridecanoic acid
	25.76	62.07	$C_{24}H_{38}O_4$	390.55	1,2-Benzenedicarboxylic acid, diisooctyl ester
	31.79	2.077	$C_{25}H_{50}O_2$	370.67	Methyl 12-methyltetradecanoate
	31.86	7.693	$C_{25}H_{50}O_2$	370.67	Methyl 12-methyltetradecanoate
EG	7.9	3.138	$C_{11}H_{11}N$	157.21	Pyrrole, 2-methyl-5-phenyl-
	8.36	31.937	$C_8H_{10}O_3$	154.16	Phenol, 2,6-dimethoxy-
	13.67	5.391	$C_{11}H_{14}O_3$	194.23	Phenol, 2,6-dimethoxy-4-[2-propenyl]-
	14.58	11.608	$C_{11}H_{14}O_4$	210.23	2-Pentanone, 1-[2,4,6-trihydroxyphenyl]
	31.82	4.181	$C_{25}H_{50}O_2$	370.67	Methyl 12-methyltetradecanoate
WT	4.16	11.130	$C_{15}H_{14}O_2$	226.28	3-Benzyl-4-methoxybenzaldehyde
	4.5	10.153	C_8H_{14}	110.20	1-Methylcyclohex-1-ene
	8.39	33.838	$C_8H_{10}O_3$	154.16	Phenol, 2,6-dimethoxy-
	11	3.158	$C_9H_{13}NO_3$	183.2	Cyclohexanone, 2-[2-nitro-2-propenyl]-
	11.2	9.586	$C_{15}H_{14}O_2$	226.28	3-Benzyl-4-methoxybenzaldehyde
	14.59	13.261	$C_{11}H_{14}O_4$	210.23	2-Pentanone, 1-[2,4,6-trihydroxyphenyl]
	31.87	18.874	$C_{25}H_{50}O_2$	370.67	Methyl 12-methyltetradecanoate
NC	4.15	4.774	$C_{16}H_{24}$	216.37	3-Phenyldecane
	7.04	1.513	$C_{20}H_{38}O_2$	310.52	Methyl 9-octadecenoate
	13.42	1.716	$C_{13}H_{16}O$	188.27	1-Benzyloxy-2,4-dimethylbenzene
	17.02	1.988	$C_{34}H_{50}O$	474.76	2,3,5,6-Tetramethylphenol
	17.94	11.916	$C_{23}H_{30}O_4$	370.48	1,4-Benzenedicarboxylic acid, 2-(decyloxy)ethyl ester
	20.65	0.929	$C_{25}H_{48}O_2$	368.66	Methyl 9-octadecenoate
	25.76	68.694	$C_{24}H_{38}O_4$	390.55	1,2-Benzenedicarboxylic acid, diisooctyl ester
	31.85	6.207	$C_{23}H_{30}O_4$	370.48	1,4-Benzenedicarboxylic acid, 2-(decyloxy)ethyl ester

The biooil obtained from HTC of *Casuarina equisetifolia L*. biomass at 250°C was analyzed to have Benzyl oxy tridecanoic acid, 1,2-Benzenedicarboxylic acid, diisooctyl ester, and Methyl 12-methyltetradecanoate. The formation of these compounds was attributed to various chemical reactions that occur during the HTC process [32]. Benzyl oxy tridecanoic acid was identified as a product of lignin degradation, while 1,2-Benzene dicarboxylic acid, diisooctyl ester, likely resulted from reactions between aromatic compounds and aliphatic alcohols or carboxylic acids[33]. Furthermore, Methyl 12-methyltetradecanoate was found to be produced through the decarboxylation of fatty acids present in the biomass [34].

The biooil obtained from the HTC of *Eucalyptus globulus* at 250°C revealed the presence of several important constituents, including Pyrrole, 2-methyl-5-phenyl-, Phenol, 2,6-dimethoxy-, and Phenol, 2,6-dimethoxy-4-[2-propenyl]-, which were likely formed through the degradation and condensation of lignin and hemicellulose components [35]. The thermal decomposition of polyphenols present in the Eucalyptus biomass resulted in the formation of 2-Pentanone, 1-[2,4,6-trihydroxyphenyl]. Furthermore, Methyl 12-methyltetradecanoate was detected, indicating the presence of fatty acids and their derivatives in the biooil [34].

The biooil resulted from the HTC of *Wrightia tinctoria* at 250°C exhibited a diverse array of constituents, including 3-Benzyl-4-methoxybenzaldehyde, 1-Methylcyclohex-1-ene, Phenol, 2,6-dimethoxy-, and Cyclohexanone, 2-[2-nitro-2-propenyl]-. These compounds are likely formed through various chemical reactions involving the breakdown and rearrangement of lignin, cellulose, and hemicellulose present in the biomass [36][37]. The detection of 3-Benzyl-4-methoxybenzaldehyde suggests the involvement of benzyl groups in the degradation processes. Furthermore, the presence of 2-Pentanone, 1-[2,4,6-trihydroxyphenyl], and Methyl 12-methyltetradecanoate indicates the presence of polyphenolic compounds and fatty acids in the biooil [34].

The biooil resulted from the HTC of *Neolamarika cadamba* at 250°C exhibited a varied range of constituents, including 3-Phenyl decane, Methyl 9-octadecenoate, 1-Benzyloxy-2,4-dimethyl benzene, 2,3,5,6-Tetramethylphenol, 1,4-Benzene dicarboxylic acid, 2-(decyloxy)ethyl ester, and 1,2-Benzene dicarboxylic acid, diisooctyl ester. The presence of 3-Phenyldecane suggests the involvement of aromatic compounds and aliphatic alcohols in the biooil formation and aging of biooil on storage [38]. Methyl 9-octadecenoate indicates the presence of fatty acids and their derivatives in the biooil [34]. Furthermore, the identification of 1-Benzyloxy-2,4-dimethylbenzene and 2,3,5,6-Tetramethylphenol implies the possible involvement of lignin degradation and the formation of phenolic compounds during the HTC process. Additionally, the presence of 1,4-Benzenedicarboxylic acid, 2-(decyloxy)ethyl

ester, and 1,2-Benzenedicarboxylic acid, diisooctyl ester may be attributed to the interaction of aromatic compounds with aliphatic alcohols or carboxylic acids during the biomass conversion.

The biooils resulted from the hydrothermal carbonization (HTC) process of various biomass sources exhibited a variety of functional groups, including benzyl, carboxylic acid, ester, methyl, phenol, pyrrole, nitro, and aliphatic hydrocarbons. These functional groups are indicative of the chemical transformations that occur during the HTC process, involving lignin degradation, esterification, condensation reactions, and decarboxylation of fatty acids. The presence of these diverse functional groups highlights the complex nature of the biooil composition and its potential for various applications in renewable energy and value-added products.

CONCLUSIONS

The hydrothermal carbonization (HTC) process was successfully applied to four different biomass sources, namely *Casuarina equisetifolia L., Eucalyptus globulus, Wrightia tinctoria*, and *Neolamarika cadamba*, at varying reaction temperatures of 180°C, 215°C, and 250°C. The results showed that HTC can effectively convert woody biomass into biooil, biochar, and biogas products. It was observed that at 180°C maximum mass yield was obtained while maximum energy intensification was achieved at 250°C. The surface morphology study confirmed that HTC changes the uniform fibrous woody biomass structure to an amorphous biochar at higher temperatures. Higher biooil yield was observed at 250°C. The biooil obtained from the HTC process exhibited a complex composition with various functional groups, including benzyl, carboxylic acid, ester, methyl, phenol, pyrrole, nitro, and aliphatic hydrocarbons. These functional groups indicate the occurrence of diverse chemical reactions during the HTC process, involving lignin degradation, esterification, and fatty acid decarboxylation. The study demonstrated that the reaction temperature significantly influenced the biooil yield and composition, with higher temperatures favoring the formation of biooil and reducing the biochar yield. Moreover, specific biomasses exhibited unique compositions of biooil constituents, indicating that the HTC process can be tailored to optimize the production of desired products from different feedstocks. Overall, this study sheds light on the potential of HTC as a promising thermochemical conversion technology for the valorization of woody biomass into valuable bio-based products and renewable energy sources.

EXPERIMENTAL SECTION

Chemical constituent analysis and proximate analysis

A typical wood or plant material consists of four basic constituents: extractives, holo-cellulose (cellulose + hemicellulose), lignin, and ash. For this study, 4 grams of oven-dried wood of particle size 0.40 mm (40 mesh) was subjected to sequential extraction using 95% ethanol, pure benzene, 98% dichloromethane, 1:2 volume mixture of ethanol-benzene, and 99.5% acetone, each for 4-5 hours using a Soxhlet extraction setup. The percentage of extractives was determined using TAPPI (T 204 cm-97) after the evaporation of residual solvent and drying for 1 hour at 105 ± 3°C, followed by cooling in a desiccator and calculated using Equation (1) [23]. The percentage of holo-cellulose and lignin was determined from the extractives-free wood sample using standard methods provided by TAPPI T 203 and TAPPI T 222 om-21 respectively [24]. The wood was extracted consecutively with 17.5% and 9.45% sodium hydroxide solutions at 25°C. The soluble fraction, consisting of beta- and gamma-celluloses, is determined volumetrically by oxidation with potassium dichromate, and the alpha-cellulose, as an insoluble fraction, is derived by difference. The acid-soluble lignin was determined in a solution, after filtering off the insoluble lignin, by a spectrophotometric method based on absorption of ultraviolet radiation at wavelength 205 nm.

$$\text{Extractives (\%)} = [(W_e - W_b)/ W_p] \times 100 \quad (1)$$

where W_e is the dry weight of extract in g, W_b is the dry weight of blank residue in g and W_p is the dry weight of the wood in g.

The proximate analysis was performed as per ASTM standards to determine volatile matter, ash, moisture, and fixed carbon present in the solid samples. The volatile matter was determined by subjecting the sample to a temperature of 950 ± 20°C for 7 minutes in a covered crucible within a muffle furnace. Subsequently, the cooled sample was placed in a desiccator for further analysis as per ASTM-E872. To ascertain the percentage ash content (in accordance with ASTM-E1755), the desiccated solid samples underwent heating at 575 ± 25°C for a duration of 3 hours in a muffle furnace. Concurrently, the percentage moisture content was determined by exposing a measured sample quantity to an air oven set at 103°C for a period of 16 hours, following ASTM-E871-82. [25]. Equation (2) was utilized to estimate the Fixed Carbon Content (FCC) as given in ASTM D3172-13.

$$\text{FCC (\%)} = 100 - (\text{\% volatile matter} + \text{\% ash} + \text{\% moisture}) \quad (2)$$

Hydrothermal carbonization and Energy intensification

HTC of woody biomass was conducted in a 50 mL non-stirred hydrothermal reactor at varying reaction temperatures (180°C, 215°C, and 250°C), maintaining a consistent reaction time of 1.5 hours. The reactor was fitted with a k-type temperature transducer to measure the internal temperature. The setup was placed inside a muffle furnace, and the furnace temperature was controlled proportionally to the internal reactor temperature. A total of 3 grams of woody biomass feedstock with 18 mL of deionized water was added to maintain a water to feedstock ratio of 6:1 (on volume to mass ratio). The initial average moisture content of the woody biomass feedstock was measured using Thermo-gravimetry to be 7.85%. The reactor was heated at a rate of 40°C/min and held for the specified reaction duration. Subsequently, rapid cooling was achieved by immersing the reactor in cold water. Once the system reached room temperature, the pressure release valve was opened, and the evolved gaseous products were collected in a 1 L Tedlar bag. Separation of solid and liquid products was accomplished using a fine mesh nylon cloth with a maximum pore size of 0.15 mm. The liquid product obtained was subjected to cooling at 15°C, followed by centrifugation to separate residual water from the bio-oil. The solid component was washed with dichloromethane, filtered through paper with a pore size of 2.5 µm, and then subjected to evaporation to gather the bio-oil mixed with solid char. The solid char was subsequently dried overnight (for a minimum of 12 hours) in an oven set at 103°C. Figure 9 illustrates the schematic diagram of the HTC process employed in this study.

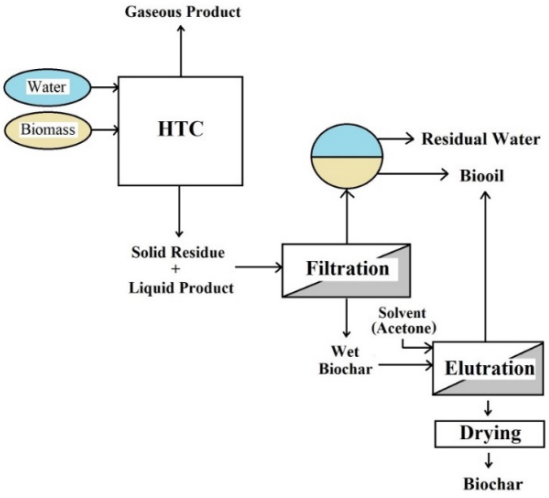

Figure 9. Schematic diagram for hydrothermal carbonization process.

The CHN Elemental analyzer (Thermo Finnigan, Italy) was employed to determine the elemental composition (C, H, and N) of both the feed and biochar samples. The oxygen content was derived by difference. The theoretical higher heating value (HHV) in MJ/kg was computed using an empirical correlation established by Channiwala and Parikh (2002) through Equation (3):

$$HHV=0.3491C+1.1783H+0.1005S-0.1034O-0.0015N-0.0211A \quad (3)$$

In this equation, C, H, S, O, N, and A denotes the weight percentages of carbon, hydrogen, sulfur, oxygen, nitrogen, and ash in solids, respectively [26].

Kambo, H. and Dutta, A. [27] pinpointed crucial parameters for hydrothermal carbonization, specifically mass yield, energy densification ratio, and energy yield. These parameters were computed using the following equations (4, 5, and 6)

$$\text{Mass yield (MY)} = M_{product} / M_{feed} \quad (4)$$

$$\text{Energy densification ratio (EDR)} = HHV_{char} / HHV_{feed} \quad (5)$$

$$\text{Energy yield (EY)} = MY / EDR \quad (6)$$

where M_product and M_feed are the mass of dried and moisture free char, oil or gas produced individually and mass of dried raw feedstock, while HHV_char and HHV_feed are the HHV of biochar (on dry basis) and HHV of raw feedstock (on dry basis).

The following correlation was used by Sermyagina, E et al. (2015) to describe the experimental results for mass yield and energy yield with satisfactory accuracy for temperature range between 180 and 250°C; calculating the constants by minimizing the RSS:

$$\text{Mass yield (MY\_Ser)} = (1-0.04079(T-150)^{0.337} t^{0.2142} r^{0.3055}) \quad (7)$$

$$\text{Energy yield (EY\_Ser)} = (1-0.05632(T-150)^{0.062} t^{0.2846} r^{0.4405}) \quad (8)$$

In the experimental study, the process temperature (T) was measured in °C, the residence time (t) was measured in hours, and the water to biomass ratio (r) was considered. The obtained experimental results from equations (3) and (4) were compared with the corresponding correlation curves obtained from equations (7) and (8). This comparison aimed to determine the similarity in the hydrothermal carbonization (HTC) of biomass that exhibited similar characteristics but with somewhat different rates [28].

To investigate the morphology of the selected biochars at different experimental temperatures (180°C, 215°C, 250°C) and magnifications (x150, x500, x2000), Scanning Electron Microscope (SEM) analysis was conducted using a Jeol JSM 6390 instrument. This analysis aimed to identify the morphological changes in the surfaces and structures of the biochar during the HTC process.

Chemical Characterization of bio-oil from HTC

To examine the liquid fraction known as bio-oil from HTC, Gas Chromatography-Mass Spectrometer (GC-MS) analysis was conducted employing Agilent 7890 with a Flame Ionization Detector (FID) and Jeol AccuTOF GCV to identify its chemical constituents. The GC-MS system included a glass column with a 0.53 mm internal diameter, 105 m length, and a film thickness of 0.25 µm. A 2 µL sample was introduced through the injector, utilizing helium as the carrier gas. The MS operated at 70 eV of ionization energy. Carrier gas column flow and purge flow were maintained at 1 mL/min and 5 mL/min, respectively, initiating with an oven temperature of 50°C, escalating to 280°C over 22 min, and held for 35 min. The mass range spanned from 45 to 300 amu, with a scan interval of 0.50 s, and the MS source temperature was set at 260 °C. The split ratio was 10:0, and the entire duration of the GC-MS analysis amounted to 65 min. The relative percentage of each component was expressed as a percentage with peak area normalization.

ACKNOWLEDGMENTS

The authors would like to extend their thanks to SAIF, IIT Bombay, the Center of Research in Nanotechnology at Karunya Institute of Technology and Sciences, Coimbatore, for their assistance in analysis and particle characterization, and Tamil Nadu Forests Department, Chennai and Mettupalayam for their guidance and support. Additionally, gratitude is expressed to the Department of Chemical Engineering, Kongu Engineering College, Perundurai, Erode, for providing the necessary infrastructure facilities and support for conducting the aforementioned research.

REFERENCES

1. J.J. Chew, V. Doshi, *Renew. Sustain. Energy Rev*., **2011**, *15*, 4212–4222.
2. B. Dou, H. Zhang, Y. Song, L. Zhao, B. Jiang, M. He, C. Ruan, H. Chen, Y. Xu, *Sustain. Energy Fuels*, **2019**, *3*, 314–342.
3. H. Chen, X. Fu, *Renew. Sustain. Energy Rev*., **2016**, *57*, 468–478.
4. B. Ercan, K. Alper, S. Ucar, S. Karagoz, *J. Energy Inst*., **2023**, *109*, 101298.

5. P. Basu, Biomass Gasification, Pyrolysis Torrefaction Pract. Des. Theory **2013**, 1–530.
6. S.S. Jamari, J.R. Howse, *Biomass Bioenerg*, **2012**, *47*, 82–90.
7. H.-G. Ramke, D. Blöhse, H.-J. Lehmann, J. Fettig, S.T. Höxter, Sardinia 2009 Twelfth Int. Waste Manag. Landfill Symp. **2009**.
8. A. Funke, F. Ziegler, *Biofuels, Bioprod. Biorefining*, **2010**, *4,* 160–177.
9. S.E. Elaigwu, V. Rocher, G. Kyriakou, G.M. Greenway, *J. Ind. Eng. Chem.*, **2014**, *20*, 3467–3473.
10. P. Regmi, J.L. Garcia Moscoso, S. Kumar, X. Cao, J. Mao, G. Schafran, *J. Environ. Manage.*, **2012**, *109*, 61–69.
11. M.A. Islam, A. Benhouria, M. Asif, B.H. Hameed, *J. Taiwan Inst. Chem. Eng.*, **2015**, *52*, 57–64.
12. H.H. Hammud, A. Shmait, N. Hourani, *RSC Adv.*, **2015**, *5*, 7909–7920.
13. S.M. Heilmann, J.S. Molde, J.G. Timler, B.M. Wood, A.L. Mikula, G. V. Vozhdayev, E.C. Colosky, K.A. Spokas, K.J. Valentas, *Environ. Sci. Technol.*, **2014**, *48*, 10323–10329.
14. N.D. Berge, L. Li, J.R.V. Flora, K.S. Ro, *Waste Manag.*, **2015**, *43*, 203–217.
15. Z. Gao, Y. Zhang, N. Song, X. Li, *Mater. Res. Lett.*, **2017**, *5*, 69–88.
16. S. van L. and J. Koppejan, ed., The Handbook of Biomass Combustion and Co-Firing, Routledge, **2012**, London.
17. M.B. Sticklen, *Nat. Rev. Genet.*, **2008**, *9*, 433–443.
18. X. Lu, P.J. Pellechia, J.R.V. Flora, N.D. Berge, *Bioresour. Technol.*, **2013**, *138*, 180–190.
19. S. Kang, X. Li, J. Fan, J. Chang, *Ind. Eng. Chem. Res.*, **2012**, *51*, 9023–9031.
20. D. Kim, K. Lee, K.Y. Park, *J. Ind. Eng. Chem.*, **2016**, *42*, 95–100.
21. S. Kamal, M.S. Hossain, I.H. Sadab, K.B. Kabir, K. Kirtania, *Fuel Commun.* **2023**, 100090.
22. M. Volpe, A. Messineo, M. Mäkelä, M.R. Barr, R. Volpe, C. Corrado, L. Fiori, *Fuel Process. Technol.*, **2020**, *206*, 106456.
23. TAPPI (*Technical Association of Pulp and Paper Industry*), T 204 C. **2007**.
24. T. Ona, T. Sonoda, M. Shibata, K. Fukazawa, *Tappi J.*, **1995**, 78,121–126.
25. P. Basu, Biomass Gasification, Pyrolysis and Torrefaction **2018**, 479–495.
26. S.A. Channiwala, P.P. Parikh, *Fuel*, **2002**, 1051–1063.
27. H.S. Kambo, A. Dutta, *Energy Convers. Manag.*, **2015**, *105*, 746–755.
28. E. Sermyagina, J. Saari, J. Kaikko, E. Vakkilainen, *J. Anal. Appl. Pyrolysis*, **2015**, *113*, 551–556.
29. S. V. Vassilev, C.G. Vassileva, V.S. Vassilev, *Fuel*, **2015**, *158*, 330–350.
30. S.E.C. Whitney, M.G.E. Gothard, J.T. Mitchell, M.J. Gidley, *Plant Physiol.*, **1999**,*121*, 657–663.
31. S. Bilgen, K. Kaygusuz, A. Sari, *Energy Sources*, **2004**, *26*, 1083–1094.
32. G. Ischia, L. Fiori, *Waste Biomass Valori.*, **2021**, *12*, 2797–2824.
33. L. Liu, Biomass-Derived Humins Form. Chem. Struct., Springer, **2023**, pp. 85–99.
34. M. do S.B. da Silva, J.G.L. de Araujo, J.C.C. V Bento, A.M. de Azevedo, C.R.O. Souto, A.S.D. dos Anjos, A.M.M. de Araújo, D.R. da Silva, F.G. Menezes, A.D. Gondim, L.N. Cavalcanti, *RSC Adv.*, **2022**, *12*, 27889–27894.

35. K. Werner, L. Pommer, M. Broström, *J. Anal. Appl. Pyrolysis*, **2014**, *110*, 130–137.
36. D. Chen, K. Cen, X. Zhuang, Z. Gan, J. Zhou, Y. Zhang, H. Zhang, *Combust. Flame*, **2022**, *242*, 112142.
37. C. Zhou, X. Xia, C. Lin, D. Tong, J. Beltramini, *Chem. Soc. Rev*., **2011**, *40*, 5588–617.
38. R. Wang, H. Ben, *Front. Energy Res*., **2020**, *8*, 1–12.